Spatial variation of the two-dimensional electron gas density induced by an increasing Hall electric field

I. Baskin, B. M. Ashkinadze, and E. Cohen
Solid State Institute, Technion–Israel Institute of Technology, Haifa 32000, Israel

V. V. Belkov
A.F. Ioffe Physical–Technical Institute, Russian Academy of Sciences, 194021 St. Petersburg, Russia

L. N. Pfeiffer
Department of Electrical Engineering, Princeton University, Princeton, New Jersey 08544, USA

V. Umansky
Braun Center for Submicron Research, Weizmann Institute, Rehovot, Israel

(Received 10 September 2011; revised manuscript received 6 December 2011; published 28 December 2011)

The local properties of a high-mobility, two-dimensional electron gas (2DEG) subjected to an increasing Hall electric field are studied by imaging photoluminescence spectroscopy. It is observed that as the Hall electric field increases, the distribution of a 2DEG density across the sample becomes spatially nonuniform. This nonuniformity is associated with the "gating effect" of the Hall electric field that is screened by low-mobility charges accumulating in the layers parallel to the 2DEG. We consider two mechanisms to explain the 2DEG density redistribution induced by the Hall electric field. The first involves in-plane electron transport that results in a linear 2DEG density variation across the Hall bar. The second is activated at a high Hall voltage (>50 mV) and involves vertical electron tunneling out of the 2DEG layer. We conclude that the 2DEG density redistribution can affect the nonlinear magnetotransport phenomena recently studied in GaAs/Al_xGa_{1-x}As heterostructures containing a high-mobility 2DEG.

DOI: 10.1103/PhysRevB.84.245320 PACS number(s): 73.43.Qt, 78.55.Cr, 78.67.De

I. INTRODUCTION

The two-dimensional electron gas (2DEG) system subjected to crossed magnetic (B) and electric field has been studied intensively since the discovery of the quantum Hall effect (QHE).[1,2] In the past few years, a number of remarkable magnetotransport phenomena were observed in a high-mobility 2DEG under increased dc current. Among these are Hall field-induced resistance oscillations,[3,4] nonlinear magnetoresistance,[5] and zero differential-resistance states.[6] The models proposed for interpreting these nonlinear phenomena[7] are usually based on the assumption that the 2DEG density n_{2D} and mobility are spatially uniform throughout the sample and thus are not affected by the increased Hall electric field (HEF), E_H.[5]

In general, charged carriers deflected by the HEF to the sample edge can lead to a spatial charge redistribution. In a three-dimensional sample (a slab), a self-consistent charge distribution is obtained by establishing charge layers on the slab edges. In the 2D Hall effect, charge, potential, and current distributions are more complicated and have been studied extensively. In the QHE regime in particular, the 2DEG density distribution was investigated theoretically[8–10] and experimentally by electro-optical potential imaging[11] and scanning inductive probe.[12] By using photoluminescence microspectroscopy, Frankenberger *et al.*[13] reported on a strong variation of the electron density across a Hall bar at high B (>4 T). The spatially nonuniform distribution of the photoluminescence intensity was observed in a current biased sample at high magnetic field.[14] These techniques gave valuable information about the current density and Hall potential distribution in the QHE regime.

A direct study of the 2DEG density distribution in high-mobility heterostructures under increased Hall electric field is timely and important because the lateral variation of the 2DEG properties can affect the nonlinear magnetotransport effects that were recently observed at low B ($\leqslant$1 T).[3–5,15]

In order to measure the local 2DEG density n_{2D}, we use an imaging photoluminescence (PL) spectroscopy. The latter measures the spatial distribution of the PL spectrum, which is due to radiative direct interband 2De-h (2D electron-photoexcited valence hole) transitions occurring in the spectral range of $\triangle E = E_{PL}(k_F) - E_0$, as shown in Fig. 1(a). Thus, $\triangle E$ is mainly determined by the electron Fermi energy, $E_F \propto n_{2D}$,[16] and imaging the PL spectrum provides an n_{2D} distribution map (as well as the 2DEG temperature T_e variation).[17,18]

We observe that with increasing E_H, the spatial 2DEG density distribution along the Hall field, $n_{2D}(y)$, becomes nonuniform. At low bias current, $n_{2D}(y)$ varies linearly with a slope proportional to the Hall voltage, $V_H = I_{dc}B/|e|n_{2D}$, where I_{dc} is the driving dc-bias current. At high Hall voltages, $n_{2D}(y)$ shows a nonlinear dependence, and the n_{2D} value, averaged over the Hall bar, decreases. We propose that the 2DEG density redistribution is caused by a "gate voltage" arising between the 2DEG and a low-mobility conductive channel in the GaAs/Al_xGa_{1-x}As heterostructure layer. Further information about the mechanisms leading to the HEF-induced n_{2D} nonuniformity is obtained in a time-resolved PL experiment. It was observed that the PL intensity transients

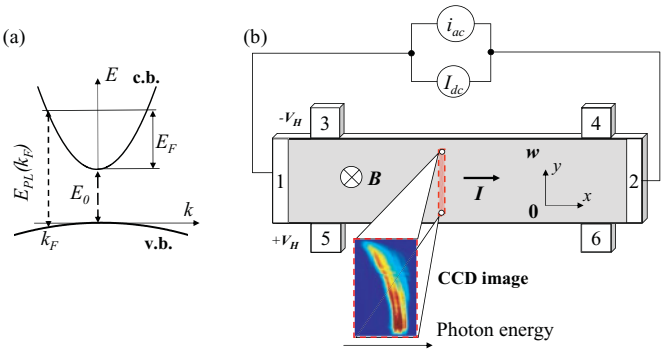

FIG. 1. (Color online) (a) Direct optical transitions due to recombination of low-density photoholes in the valence band (v.b.) and 2D electrons in the conduction band (c.b.). E_F is the electron Fermi energy, and the emitted photon energies are in the range of $\triangle E = E_{\rm PL}(k_F) - E_0$. (b) A schematic description of the Hall bar and the spatially resolved photoluminescence experiment.

induced by short (10–100-μs duration) current pulses have fast and slow components in the 2DEG density redistribution, corresponding to different mechanisms of modulation of n_{2D}.

II. EXPERIMENTAL DETAILS

We studied several Hall bar samples that were fabricated from GaAs/Al_xGa_{1-x}As heterostructures containing a high-mobility 2DEG. The heterostructures were grown by molecular beam epitaxy on (001)-GaAs wafers. Each one contains a single modulation-doped GaAs/Al_xGa_{1-x}As quantum well (MDQW) whose width was in the range of 20–40 nm. The Si-doped layer is located either asymmetrically (single-side doping) or symmetrically (two-side doping) with respect to the QW, and is separated from it by an Al_xGa_{1-x}As spacer with a width of 50–100 nm (depending on the doping level). The nominal 2DEG density, n^0_{2D}, and mobility, μ_e, were measured independently and are in the range of (1.0–3.6) $\times$ 10^{11} cm^{-2} and (2–15) $\times$ 10^6 cm^2/V s, respectively.[19,20]

In our spatially resolved (imaging) PL spectroscopy technique, a laser beam was focused to form a vertical illuminated strip (2 mm high and 0.2 mm wide) on the sample surface [as shown schematically in Fig. 1(b)] The luminescence from the photoexcited strip was optically magnified and imaged on the spectrometer slit, dispersed in the horizontal direction and projected on a CCD matrix. Thus, the image on the CCD plane provides both spatial (in the direction across the sample) and spectral resolution with a corresponding spatial resolution of $\approx$0.01 mm and a spectral resolution of 0.1 meV. A laser diode with a photon energy of $E_L = 1.56$ eV (below the Al_xGa_{1-x}As barrier band gap) or a He-Ne laser of low intensity were used for photoexcitation so that the 2DEG density in the illuminated area was very close the nominal n^0_{2D} value measured in the dark (in transport study). An external magnetic field, $B < 1$ T, was applied normally to the 2DEG layer. The sample was immersed in liquid He at a temperature of $T_L = 2$ K.

Hall bars of size $\approx 5 \times 1$ mm^2 were prepared either by standard lithography or by cleaving rectangular bars and subsequent soldering In/Sn alloy contacts to the 2DEG layer. Magnetoresistance measurements were performed with a standard lock-in technique at a frequency of 17 Hz and a low ac current (of 0.1 μA). The ac and dc (bias) current, $i_{\rm ac}$ and $I_{\rm dc}$, respectively, were driven through the edge contacts [numbered 1 and 2 in the scheme of Fig. 1(b)], and the longitudinal voltage was measured on contacts 3–4. The dc current varied in the range of 5–300 μA. The Hall voltage was measured on contacts 3 and 5. The 2DEG density, n^0_{2D}, was obtained from the period of the SdH resistance oscillations. This period does not change under weak laser illumination with the intensity, $I_L < 10$ mW/cm^2, and n^0_{2D} was found to be very close to the nominal value.

The temporal evolution of the HEF-induced PL modulation was studied by applying current pulses of 10–100 μs duration (the pulse rise and fall times <1 μs). The time-resolved PL signal was detected by a cooled photomultiplier, having a response time of 2 ns, and measured with a gated photon counter. The spatial resolution in the time-resolved measurements was obtained by introducing a pinhole mask on the spectrometer entrance slit so that the PL transients are measured near the Hall bar edge ($y \simeq 0$).

III. RESULTS

Although the PL images turn out to be dependent on the particular sample heterostructure, size, and n^0_{2D}, similar HEF-induced effects were observed in all the studied samples. Figure 2 shows typical results obtained for a 30-nm-wide MDQW specimen with $n^0_{2D} = 3.6 \times 10^{11}$ cm^{-2} and mobility above 2×10^6 cm^2/V s. Four series of PL spectra are shown, measured across the Hall bar (namely, along the Hall field direction, y) under an applied magnetic field of $B =$ 0.35 and 0.7 T. For $I_{\rm dc} = 0$, the PL spectra are spatially

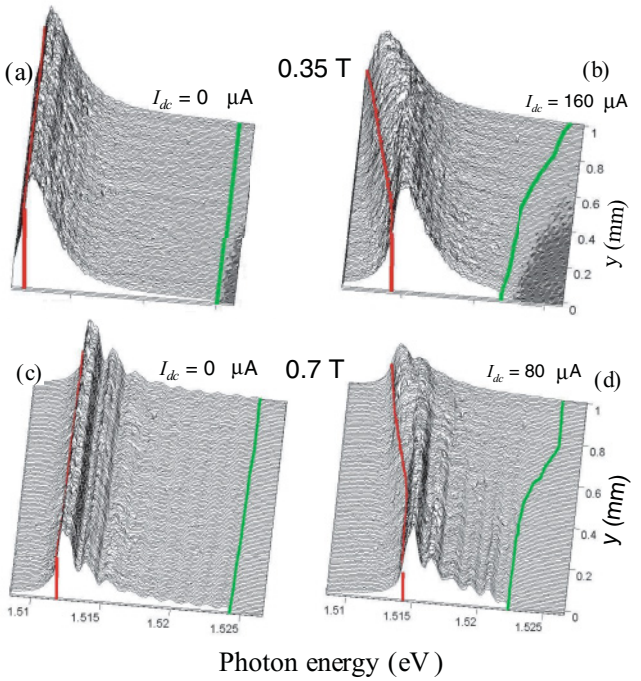

FIG. 2. (Color online) Spatially resolved PL spectra measured on a Hall bar with a nominal $n_{2D} = 3.6 \times 10^{11}$ cm^{-2} at $T_L = 2$ K and under $B = 0.35$ and 0.7 T. (a),(c) $I_{\rm dc} = 0$; (b),(d) $V_H \approx 100$ mV at $I_{\rm dc} = 160$ A and 80 μA, respectively. The red and green curves mark the PL onset and $E_{\rm PL}(k_F)$ energy, respectively.

uniform [Figs. 2(a) and 2(c)], and the PL spectral bandwidth $\triangle E = E_{\rm PL}(k_F) - E_0$ corresponds to the nominal 2DEG density ($n^0_{\rm 2D}$ measured in the dark). The dc current induces significant variations in the PL spectra across the Hall bar [Figs. 2(b) and 2(d)]: In the region of high Hall potential (near $y \sim 0$), the low-energy PL onset E_0 shifts to a higher energy, the spectral bandwidth $\triangle E$ decreases, and the PL peak intensity increases.

Both the blueshift (of E_0) and the decrease in $\triangle E$ indicate a decreased $n_{\rm 2D}$ value in the direction of the increased Hall potential. Indeed, the E_0 shift results from the band-gap renormalization (BGR) effect occurring at high $n_{\rm 2D}$.[21] The high-energy, steplike PL intensity decrease occurs at $E_{\rm PL}(k_F)$, corresponding to the valence hole recombination with 2D electrons at the Fermi vector k_F. In the wide MDQW's studied here, the valence hole dispersion effect on the emitted photon energy can be neglected, and $E_F(y) = \triangle E(y)$. Then, the local 2DEG density value is obtained: $n_{\rm 2D}(y) \simeq E_F(y)/D_e$, where $D_e = \pi\hbar^2/m^*_e$ is the averaged 2D electron density of states, which has the value of $D_e = 3.5 \times 10^{-11}$ meV/cm^{-2} for GaAs.

The total 2DEG PL intensity (energy-integrated PL), measured at each y point, remains unchanged with increasing Hall field. This means that the 2De-h radiative recombination rate is not affected by the Hall field, and therefore the Hall electric field does not affect the local density of the photoholes. It should be noted that a similar spatially nonuniform PL distribution across the Hall bar (along the y direction) was observed as the laser-illuminated strip was moved along the x direction.

At higher B (above 0.5 T), distinct bands due to the 2De-h recombination between the Landau levels (LL's) emerge in the PL spectra. At $B = 0.7$ T [Figs. 2(c) and 2(d)], nine LL PL bands are seen, and the spectrum at $I_{\rm dc} = 0$ does not vary in the y direction. The LL separation is $\approx$1.3 meV, which is close to the electron Larmor energy at this magnetic field, $\hbar eB/m^* = 1.2$ meV. Under dc bias, the PL spectra in Fig. 2(d) show spatial variations along the y direction that are similar to those displayed in Fig. 2(b). At $B = 0.7$ T, the total number of occupied LL's and the PL spectral width, ΔE, decrease toward $y \sim 0$. In this case, $E(k_F)$ can be accurately measured from the energy of the highest LL PL band.

The $n_{\rm 2D}$ dependence on the Hall-induced voltage V_H was studied by measuring the PL spectrum near $y \sim 0$ at different $I_{\rm dc}$ and B values. The PL spectra displayed in Fig. 3 were obtained for $V_H = 0$, $+75$, and -75 mV. The PL spectra measured at $B = 0.35$ and 0.7 T under the same V_H show the same energy shifts and the same spectral broadening. We conclude that the Hall-induced 2DEG density change depends on a single parameter: $V_H \propto BI_{\rm dc}$, both on its value and sign.

The local $n_{\rm 2D}$ value increases at $V_H = -75$ mV (Fig. 3, top panel), and each LL PL band broadens relative to its width at $V_H = 0$ and 75 mV. By comparing Figs. 2(c) and 2(d), one can see that the LL widths vary across the Hall bar so that the LL PL band separation is almost smeared out near $y \sim 1$, when bias current is applied. This finding definitely indicates that the effective electron temperature T_e increases under high ($-V_H$) values and varies across the Hall bar. Our detailed study of the T_e inhomogeneity generated by a high Hall electric field will be discussed elsewhere.

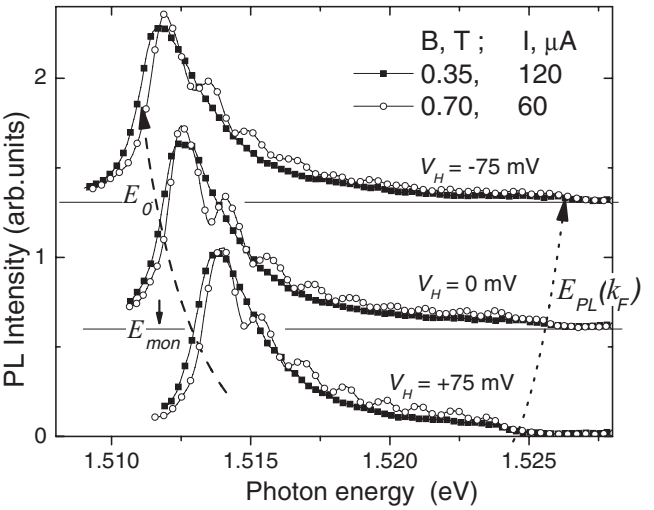

FIG. 3. PL spectra measured near the Hall bar edge ($y = 0$) for several Hall voltages. Negative V_H values correspond to the ($-x$) dc current direction. Nominal $n_{\rm 2D} = 3.6 \times 10^{11}$ cm^{-2}, $T_L = 2$ K. E_0 (estimated at a PL half-maximum intensity) and $E(k_F)$ are shown by dashed and dotted lines, respectively.

PL imaging was performed for various dc currents and several B values, and the PL spectral width dependence on y was measured. Figure 4(a) shows the $n_{\rm 2D}(y)$ values extracted from the measured $\triangle E(y)$ dependencies at various Hall voltages. For $|V_H| < 25$ mV, $n_{\rm 2D}$ shows an approximately linear y-dependence for both positive and negative V_H. The density remains nearly unchanged in the middle of the sample ($y \approx 0.5$ mm). For $|V_H| > 100$ mV, $n_{\rm 2D}(y)$ varies nonlinearly and it depends on V_H sign reversal [dashed curves in Fig. 4(a)]. In addition, the average $n_{\rm 2D}$ value decreases at high $|V_H|$.

Figure 4(b) shows the dependence of $n_{\rm 2D}$ on the Hall voltage, as obtained from the measured $\Delta E(V_H)$ at $y \sim 0$, near the Hall bar edge. In the range of $-25 < V_H < 50$ mV, the $n_{\rm 2D}(V_H)$ dependence is nearly linear, $n_{\rm 2D} = n^0_{\rm 2D} + \delta n$, where $\delta n = cV_H$ and $c \simeq -7 \times 10^8$ cm^{-2} [mV]$^{-1}$. Thus at $V_H = 25$ mV, the total variation of the density across the bar is of 10% $n^0_{\rm 2D}$, as seen in Fig. 4(a). For $V_H < -30$ mV, $n_{\rm 2D}$ saturates at 3.9×10^{11} cm^{-2}.

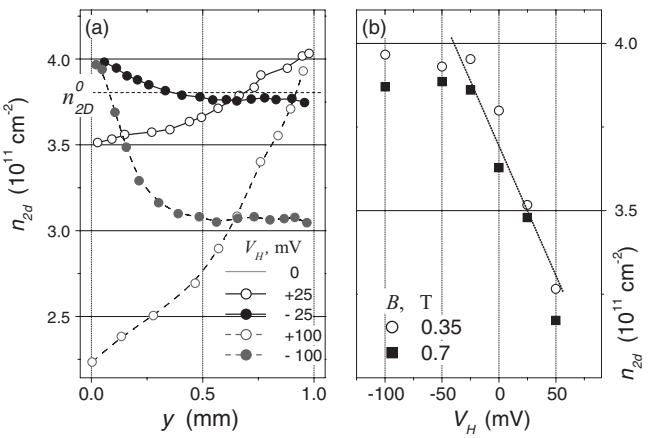

FIG. 4. (a) $n_{\rm 2D}(y)$ (along the Hall electric field) for several V_H values; (b) $n_{\rm 2D}$ ($y = 0$) as a function of the V_H. The $n_{\rm 2D}$ values are extracted from the PL spectra.

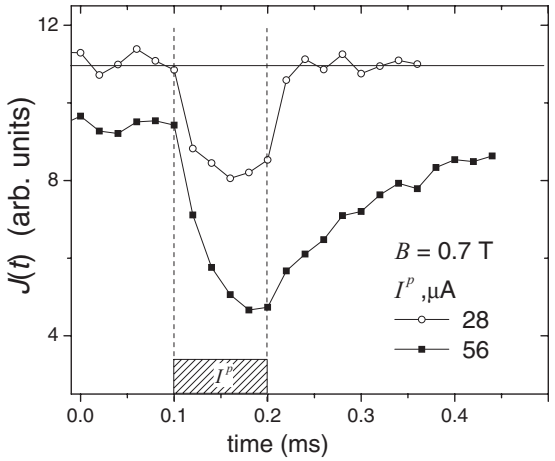

FIG. 5. Time-resolved PL intensity, J, probed at $E_{\rm mon} = 1.512$, near $y = 0$.

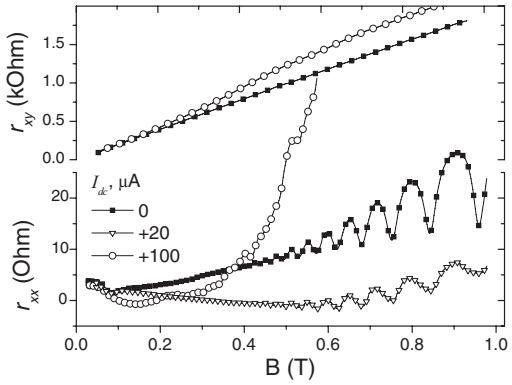

FIG. 6. Differential Hall (r_{xy}) and longitudinal (r_{xx}) magnetoresistance at various $I_{\rm dc}$ values, $T_L = 2$ K.

It is important to note that the PL spectral modification induced by increasing V_H was independent of the photoexcitation diode-laser intensity (below 20 mW/cm^2). Moreover, a similar n_{2D} spatial dependence was also observed at a lattice temperature 77 K.[22]

Additional information about the nonuniform spatial 2DEG distribution was obtained by studying the PL response to current pulses I^p. Transient traces of the PL intensity, $J(t)$, monitored at $E_{\rm mon} = 1.512$ eV (indicated by an arrow in Fig. 3), were measured at current pulses of 0.1 ms duration and a repetition rate of 0.5 kHz. Figure 5 displays $J(t)$ traces obtained near the Hall bar edge ($y = 0$) for two I^p values and $B = 0.7$ T. At the leading edge of the current pulse (Hall field increases), $J(t)$ drops due to the PL spectral blueshift caused by 2DEG depletion (see Figs. 2 and 3), and thus the n_{2D} variation with time is probed. At $I^p = 28\ \mu$A, $J(t)$ drops and recovers (after the current pulse turns off) with a characteristic time $\leqslant$0.05 ms. At high current pulses ($I^p = 56\,\mu$A), however, a much longer J-recovery time (exceeding the time interval between the current pulses, 2 ms) is detected. Such a slow recovery indicates that another mechanism is responsible for the n_{2D} redistribution at high V_H values, which is different from the n_{2D} redistribution occurring at low V_H.

The 2DEG transport properties are also affected by an increased dc bias current. At $I_{\rm dc} = 0$, the differential longitudinal and Hall magnetoresistances, r_{xx} and r_{xy}, respectively, are shown in Fig. 6 (square symbols). These B dependencies are typical of those observed in a high-mobility 2DEG. The asymmetry of the SdH oscillations and the increased r_{xx} with B are attributed to the presence of a parallel low-conductivity channel in this particular sample. Under a moderate current ($I_{\rm dc} = 20\ \mu$A, triangle symbols), a significant decrease in r_{xx} is observed at $0.2 < B < 0.6$ T, and the amplitude of SdH oscillations decreases.[5]

At $I_{\rm dc} = 100\ \mu$A, r_{xx} sharply grows with increasing B, and a longitudinal voltage instability develops at $V_H > 500$ mV (not shown). Simultaneously, a deviation from the linear r_{xy} dependence on B is observed. Similar r_{xx} changes were recently discussed in detail.[5,6] We note that the transport properties were nearly independent of the low photoexcitation intensity used (see above), and there are no observable changes in the SdH oscillation amplitudes and frequency.

IV. MODEL

The experimental results shown in Fig. 2 reveal a nonuniform distribution of the 2DEG across the Hall bar for finite dc bias current under low magnetic field $B < 1$ T. In the following, we will show that this spatially nonuniform electron density distribution arises from screening of the HEF by low-mobility charges in the layers parallel to the 2DEG, thus it is due to a "gating effect."

The spatial distribution of electrons under the Hall effect was considered in the past.[8–10] In the 3D case, the electron density distribution is uniform across the Hall bar, except for a relatively small density change at the sample edges.[10] For a 2DEG sheet embedded in an infinite dielectric medium, the Hall electric field $E_y(y)$ induces strong electron density variation within the screening length $\sim$10 nm near the Hall bar edges ($y = 0$ and $y = W$).[8,10] In the rest of the sample, the 2DEG is nearly uniform.

A significant 2DEG density nonuniformity across the Hall bar can be induced if an additional screening of the Hall electric field is provided by a conductive layer ("gate") located parallel to the 2DEG.[9] In this case, the potential of the "gate" remains constant while the Hall-induced voltage appears between the "gate" and the 2DEG layers. The existence of a parallel conductive layer has already been considered for interpreting the "anomalous" magnetoresistance[23,24] and in the experiments with increased dc bias current.[11,14]

The distribution of $n_{2D}(y)$ and $E_y(y)$ in a system consisting of the 2DEG layer and a "gate" layer separated by an undoped spacer ($Al_xGa_{1-x}As$) of thickness d_l can be obtained self-consistently from the potential distribution in the 2DEG layer relative to the "gate" one that is at zero potential:

$$\phi(y) = -|e|/C_e\left[n_{2D}^0 + \delta n(y)\right], \qquad (1)$$

where the capacitance of the 2DEG and "gate" layers $C_e = \varepsilon_0\varepsilon_{Al_xGa_{1-x}As}/d_l$ and $d_l \ll W$ (W is the Hall bar width). Hence, we have

$$E_y = -d\phi(y)/dy = |e|/C_e d(\delta n)/dy.$$

On the other hand, $E_y = E_x \mu B$, since $j_y = \sigma_{xx} E_y + \sigma_{xy} E_x = 0$ and $\sigma_{xy}/\sigma_{xx} = \mu B$ holds at low B. Here, σ_{xx} and σ_{xy} are components of the conductivity tensor. Thus, the Hall electric field is homogeneous across the sample and $E_y = V_H/W$. Then, $\delta n(y)$ depends linearly on y (implying conservation of the entire 2DEG charge),

$$\delta n(y) = V_H C_e/|e|(y - W/2)/W. \quad (2)$$

Thus, a "gate" layer gives rise to a lateral, linear variation of n_{2D}, and the entire 2DEG density modulation across the Hall bar is equal to $V_H C_e/|e|$. We note that a similar density modulation can be obtained by considering a uniform distribution of the electrochemical potential.[9,10]

The steady-state 2DEG density redistribution [Eq. (2)] that results from a HEF screening occurs with a characteristic time $\tau_{sc} \approx \rho_b C_e W^2$ (a charging time in our model). Here, ρ_b is the "gate layer" resistivity. The longest $\tau_{sc} \sim 1$ s can be estimated for a GaAs/Al_xGa_{1-x}As heterostructure where the parallel conductance is due to a high-resistivity GaAs cap layer ($\rho_b \sim 2\ G\Omega/\square$),[13] $C_e \simeq 2$ nF/cm^2 (calculated for a thin $Al_xGa_{1-x}As$ spacer, $d_l = 50$ nm), and $W = 1$ mm. This estimation shows that the gating effect takes place even for a very low (dark) parallel conductivity, and therefore the HEF-induced *in-plane* electron redistribution should be accounted for in the dc transport experiments with the increased bias current.

V. DISCUSSION

From the PL spectral measurements, we obtain that the $n_{2D}(y)$ depends nearly linearly on V_H at Hall voltages below 50 mV, and is symmetric with respect to V_H sign inversion, so that the integrated 2DEG density does not change [Figs. 4(a) and 4(b)]. Indeed, at the sample edge ($y = 0$), the 2DEG density variation is $\delta n(V_H) \approx -7 \times 10^{11} V_H$ [Fig. 4(b)]. According to Eq. (2), such a 2DEG density dependence on V_H can be affected by an "effective gate" located at a distance of $d_l = 50$ nm from the 2DEG layer. The results shown in Figs. 2–5 were obtained for the sample structure with a parallel conductive channel formed by a Si-doped layer. From Fig. 6, we estimate the latter conductivity is of 0.1–1.0 M$\Omega/\square$. Then, the characteristic HEF screening time is short enough ($\tau_{sc} \sim 0.1$–1 ms), and the 2DEG (*in-plane*) redistribution took place.

At higher $|V_H|$, an asymmetry in the $n_{2D}(y)$ distribution accompanied by an integrated 2DEG density reduction is observed [Fig. 4(a)]. These effects are due to the *vertical* electron transport (tunneling) from the MDQW to adjacent layers. The local tunneling rate strongly increases as the 2DEG potential elevates relative to the gate (along with the local n_{2D} increase). The tunneling gives rise to a nonlinear, asymmetric $n_{2D}(y)$ distribution [Fig. 4(b)] with the local density saturation at one Hall bar edge (at $|V_H| > 50$ mV) and a strong depletion at another. Thus, the integrated electron density in the 2DEG layer decreases. The 2DEG distribution asymmetry observed under the dc-current inversion [Fig. 4(a)] probably results from a spatially dependent vertical electron transport due to the inhomogeneity of barrier layer properties. In the past, a 2DEG density reduction was reported in samples subjected to intense microwave irradiation[25] or high dc current.[26]

The time-resolved PL response to current pulses measured near $y = 0$ (shown in Fig. 5) supports the two mechanisms (*in-plane* and *vertical*) for n_{2D} modulation. At low Hall voltage (current of 28 μA), a fast *in-plane* n_{2D} redistribution with a relaxation time of ~0.05 ms is observed, and this relaxation time is close to the τ_{sc} value.

At high Hall voltage (current of 56 μA, filled circles in Fig. 5), the PL relaxation time (after the termination of the pulse) increases, indicating a slow 2DEG density recovery process. This time-dependent 2DEG density modulation can be explained by a vertical electron transport between the 2DEG and the adjoining layers. Indeed, such a transport occurring during the strong V_H pulse leads to a total charge reduction in the 2DEG layer. Then, very slow vertical electron transport[27] takes place between the pulses, recovering the 2DEG density with a characteristic time of $\tau^R \sim 2$ ms.

Equation (2) allows one to estimate the maximal magnetic field and dc current values at which only slight 2DEG density nonuniformity, across the whole Hall bar, is produced by the induced HEF. For example, $\delta n/n^0_{2D}$ does not exceed 5% at $I_{dc}B < 3$ (μA T) for the structure considered above ($d_l = 50$ nm, $n^0_{2D} = 3.6 \times 10^{11}$ cm^{-2}). These maximal current and magnetic-field values are independent of the sample width and are below the corresponding I_{dc} and B values used in the recently reported nonlinear magnetotransport experiments.[5,15]

The similar 2DEG density redistributions were also observed for many studied samples in which there was no defined parallel conductive layer. In this case, photocarriers generated in the barrier layers can also contribute to the parallel conductivity channel. However, no change in the PL patterns was observed when photoexcitation intensity was reduced by three orders of magnitude (as compared with that used in the measurements shown in Fig. 2). Thus, all these observations show that there is always some low conductive parallel layer that leads to a HEF screening.

VI. CONCLUSION

Using a spatially resolved photoluminescence technique, we show that in high-quality, modulation-doped GaAs/$Al_xGa_{1-x}As$ quantum wells, a gradient in the 2D electron density along the Hall field is induced by the increased dc bias current at low magnetic field. We attribute this Hall field-induced density nonuniformity to an effective gating due to a conductive layer parallel to the 2DEG. Two mechanisms for the electron redistribution are considered: (a) In-plane electron transport leading to linear 2DEG density variation across the Hall bar with a gradient that is proportional to the Hall electric field. (b) Vertical electrical transport that is activated at higher Hall voltage, resulting in a local 2DEG density saturation and accompanied by the total charge reduction in the 2DEG layer. We propose that the Hall-induced spatially nonuniform 2DEG distribution should be taken into account in cases in which the heterostructure is driven into the nonlinear regime by increasing the Hall electric field.

ACKNOWLEDGMENTS

The work was done at the Barbara and Norman Seiden Center for Advanced Optoelectronics at Technion. It was

supported by the Israel-US Binational Science Foundation (BSF), Jerusalem and by a grant from the Ministry of Sciences and Technology, Israel and the Russian Foundation for Basic Research, the Russian Federation.

[1]K. V. Klitzing, G. Dorda, and M. Pepper, Phys. Rev. Lett. **45**, 494 (1980); D. C. Tsui, H. L. Störmer, and A. C. Gossard, *ibid.* **48**, 1559 (1982).

[2]T. Chakraborty and P. Pietiläinen, *The Quantum Hall Effects: Integral and Fractional* (Springer-Verlag, New York, 1995).

[3]C. L. Yang, J. Zhang, R. R. Du, J. A. Simmons, and J. L. Reno, Phys. Rev. Lett. **89**, 076801 (2002).

[4]W. Zhang, H.-S. Chiang, M. A. Zudov, L. N. Pfeiffer, and K. W. West, Phys. Rev. B **75**, 041304(R) (2007).

[5]S. Vitkalov, Int. J. Mod. Phys. B **23**, 4727 (2009), and references therein.

[6]A. A. Bykov, J. Q. Zhang, S. Vitkalov, A. K. Kalagin, and A. K. Bakarov, Phys. Rev. Lett. **99**, 116801 (2007).

[7]M. G. Vavilov, I. L. Aleiner, and L. I. Glazman, Phys. Rev. B **76**, 115331 (2007).

[8]A. H. MacDonald, T. M. Rice, and W. F. Brinkman, Phys. Rev. B **28**, 3648 (1983).

[9]V. M. Pudalov and S. G. Semenchinskii, JETP Lett. **42**, 232 (1985).

[10]A. Shik, J. Phys. Condens. Matter **5**, 8963 (1993).

[11]R. Knott, W. Deitsche, K. von Klitzing, K. Eberl, and K. Ploog, Semicond. Sci. Technol. **10**, 117 (1995); P. F. Fontein, J. A. Kleinen, P. Hendriks, F. A. P. Blom, J. H. Wolter, H. G. M. Lochs, F. A. J. M. Driessen, L. J. Giling, and C. W. J. Beenakker, Phys. Rev. B **43**, 12090 (1991).

[12]E. Yahel, A. Palevski, and H. Shtrikman, Superlatt. Microstruct. **22**, 537 (1997).

[13]J. Frankenberger, A. Zrenner, M. Bichler, and G. Abstreiter, Phys. Rev. B **65**, 165307 (2002).

[14]V. Novak, P. Svoboda, S. Kreuzer, W. Wegscheider, and W. Prettl, Phys. Rev. B **64**, 165302 (2001).

[15]A. T. Hatke, M. A. Zudov, L. N. Pfeiffer, and K. W. West, Phys. Rev. B **83**, 081301(R) (2011), and references therein.

[16]G. A. Bastard, *Wave Mechanics Applied to Semiconductor Heterostructures* (Halsted, New York, 1991).

[17]B. M. Ashkinadze, E. Linder, E. Cohen, and L. N. Pfeiffer, Phys. Rev. B **74**, 245310 (2006).

[18]I. Baskin, B. M. Ashkinadze, E. Cohen, and L. N. Pfeiffer, Phys. Rev. B **78**, 195318 (2008).

[19]V. Umansky, M. Heiblum, Y. Levinson, J. Smet, J. Nuebler, and M. Dolev, J. Cryst. Growth **311**, 1658 (2009).

[20]D. R. Luhman, W. Pan, D. C. Tsui, L. N. Pfeiffer, K. W. Baldwin, and K. W. West, Physica E **40**, 1059 (2008).

[21]D. A. Kleinman and R. C. Miller, Phys. Rev. B **32**, 2266 (1985).

[22]At 77 K, n_{2D} cannot be estimated from the PL spectrum due to smearing the Fermi-Dirac 2DEG distribution, however the PL spectral shift due to BGR was detected.

[23]J. Zhu, H. L. Stormer, L. N. Pfeiffer, K. W. Baldwin, and K. W. West, Phys. Rev. B **61**, R13361 (2000).

[24]S. Luryi and A. Kastalsky, Appl. Phys. Lett. **45**, 164 (1984).

[25]B. M. Ashkinadze and V. I. Yudson, Phys. Rev. Lett. **83**, 812 (1999).

[26]J. Pozela, K. Pozela, V. Juciene, and A. Shkolnik, Semicond. Sci. Technol. **26**, 01425 (2011).

[27]G. C. Kerridge *et al.*, Solid State Commun. **109**, 267 (1999).